Noise model of hyperspectral imaging system and influence on radiation sensitivity

WANG Jianyu[1], **WANG Yueming**[2], **LI Chunlai**[2]

1. *Chinese Academy of Sciences Shanghai Branch*, *Shanghai* 200083, *China*;
2. *Shanghai Institute of Technical Physics*, *Chinese Academy of Sciences*, *Shanghai* 200083, *China*

Abstract: The application effect of the hyperspectral imaging system heavily relies on the signal to noise ratio. According to design features of hyperspectral imaging system and source of various noises, various noise models are established like time-domain noise, spatial-domain noise, spatial interference, spectrum superposition and so on and the influence and restriction of various noises on hyperspectral imaging system are analyzed in detail on this basis. The conclusion of this paper plays an important role in promoting the practicability of the hyperspectral imaging system in China.

Key words: hyperspectral, radiation sensitivity, noise model

CLC number: TP702 **Document code:** A

Citation format: Wang J Y, Wang Y M and Li C L. 2010. Noise model of hyperspectral imaging system and influence on radiation sensitivity. *Journal of Remote Sensing*. **14**(4): 607—620

1 THEORETICAL MODEL FOR CALCULATING RADIATION SENSITIVITY OF HYPERSPECTRAL IMAGER

The main technical indexes for evaluating hyperspectral imager include spectral resolution, spectral coverage, spatial resolution, spatial coverage, radiation sensitivity and so on. These indexes are mutually restrictive (Tong *et al*., 2006). Radiation sensitivity is the key to successful design of the imaging system after the requirements of the spectral resolution coverage and the spatial resolution coverage are satisfied.

This paper discusses in detail the influence and restriction of various noises on the system radiation sensitivity, and especially makes in-depth study on the influence of noise in spatial domain, signal interference in spectral domain and inconsistency of different wavebands on the system radiation sensitivity through analysis on radiation characteristics of ground object and radiation sensitivity equations.

1.1 Radiation characteristics of object

Radiation of ground object consists of thermal radiation given off by the object and reflection of solar radiation. In the visible and SWIR bands (0.4—2.5μm), the radiant energy of object mainly comes from the reflection of solar radiation and its own thermal radiation is relatively small which always can be ignored during calculation. While in the mid-wave (3.0—5.0μm) and long-wave (8.0—12.5μm) thermal infrared bands, the reflected energy from solar radiation is relatively small and the radiation of object is mainly thermal radiation given off by itself. For ground object with characteristic of Lambertian reflector and the resistivity of $\rho(\lambda)$, the radiation power $P(\lambda)$ per wavelength which is absorbed by detector of hyperspectral imager in visible band and SWIR band can be expressed as follows (Yu, 1995):

$$P(\lambda)=\frac{\pi D_0^2}{4}\times\beta^2\times\tau_{\mathrm{o}}(\lambda)\times \left(\frac{1}{\pi}E(\lambda)\sin\theta\rho(\lambda)\tau_{\mathrm{a}}(\lambda)+L_{\mathrm{a}}(\lambda)\right) \tag{1}$$

where $E(\lambda)$ represents the solar spectral irradiance at the ground surface; $\tau_{\mathrm{a}}(\lambda)$ is the spectral transmittance of the atmosphere; $\tau_{\mathrm{o}}(\lambda)$ is total transmittance of optical system; θ represents sun elevation angle; $L_{\mathrm{a}}(\lambda)$ is path radiance caused by atmospheric scattering; D_0 is optical effective aperture of the spectrometer and β is instantaneous field of view (IFOV). In order to simplify the calculation, influence of path radiance $L_{\mathrm{a}}(\lambda)$ caused by atmospheric scattering is ignored.

With regard to thermal radiation of the object, the object and background of imaging system are mutual. What affect the radiation images are pixel temperature T, specific emissivity ε, reflectivity ρ, the temperature difference of adjacent pixels ΔT, the specific detectivity difference $\Delta\varepsilon$ and the reflectivity variance $\Delta\rho$. The radiation power difference per wavelength of adjacent pixels $\Delta P(\lambda)$ can be expressed as (Xue, 1992):

$$\Delta P(\lambda)=\frac{1}{4}D_0^2\beta^2\tau_{\mathrm{a}}(\lambda)\tau_{\mathrm{o}}(\lambda)\times \left(\varepsilon(\lambda)\frac{\partial L_{\mathrm{T}}(\lambda)}{\partial T}\Delta T+L_{\mathrm{T}}(\lambda)\Delta\varepsilon(\lambda)\right) \tag{2}$$

Received: 2010-02-05; **Accepted**: 2010-05-01

Foundation: Knowledge Innovation Program of the Chinese Academy of Sciences.

First author biography: WANG Jianyu (1959—), male, Professor. He holds doctor degree in Shanghai Institute of Technical Physics, Chinese Academy of Sciences. He is interested in hyperspectral imaging system design and laser active remote sensing. E-mail: jywang@mail.sitp.ac.cn

where, $L_T(\lambda)$ represents the spectral emissivity of the object.

1.2 Calculating formula of radiation sensitivity of hyperspectral imager

For the hyperspectral imager with spectral range of 0.4—2.5μm, detection sensitivity can be expressed by signal to noise ratio SNR or noise equivalent reflectance difference NE$\Delta\rho$. NE$\Delta\rho$ represents the reflectance difference of object in the case that SNR equals 1.

1.2.1 SNR calculation based on D-Specific detectivity method*

SNR calculation based on D^* method is to calculate SNR with specific detectivity of detector. This method is more suitable for traditional hyperspectral imager with single or multi-photoconductive detector. For a waveband whose central wavelength is λ and the narrow spectral bandwidth is $\Delta\lambda$, the SNR can be expressed as (Xue, 1992):

$$\mathrm{SNR}(\lambda)=\frac{V_S(\lambda)}{V_N(\lambda)}=\frac{D_0^2\beta^2\delta_e}{4\sqrt{A_d\Delta f}}\times \tau_a(\lambda)\tau_o(\lambda)D^*(\lambda)E(\lambda)\sin\theta\rho(\lambda)\Delta\lambda \quad (3)$$

where, $\tau_o(\lambda)$, $\tau_a(\lambda)$, $D^*(\lambda)$, $E(\lambda)$ and $\rho(\lambda)$ are the average value within the spectral bandwidth $\Delta\lambda$; δ_e represents the signal process factor; V_N is the noise voltage of the detector; $D^*(\lambda)$ is the normalized spectral detectivity or specific detectivity; A_d is the pixel size of the detector and Δf is noise bandwidth of the electronics.

1.2.2 SNR calculation based on quantum efficiency-equivalent electron method

Equivalent electron method is to calculate SNR through calculation of the signal electrons and noise electrons generated by the detector. This method is more applicable to hyperspectral imager with CCD detector or infrared focal plane array detector. With this method, the radiation power $P(\lambda)$ received by the detector pixel is converted to photon number $N_P(\lambda)$. The number of electrons $N_S(\lambda)$ generated by detector can be obtained with detector spectral quantum efficiency $\eta(\lambda)$. Thus, the system SNR is the ratio of signal electrons number to the sum of various noise electrons number $N_{total}(\lambda)$, which can be expressed as:

$$\mathrm{SNR}(\lambda)=\frac{N_s(\lambda)}{N_{total}(\lambda)} \quad (4)$$

where signal electrons number $N_S(\lambda)$ can also be expressed as:

$$N_s(\lambda)=N_P(\lambda)\eta(\lambda)=\frac{P(\lambda)T_{int}\lambda}{hc}\eta(\lambda) \quad (5)$$

where h represents Planck constant; c is velocity of light and T_{int} is the integration time of detector. According to Eq.(1), Eq.(4) and Eq.(5), SNR can be given by:

$$\mathrm{SNR}=\frac{N_s(\lambda)}{N_{total}(\lambda)}=\frac{D_0^2\beta^2\sin\theta T_{int}}{N_{total}\times 4hc}\times \int_{\lambda_1}^{\lambda_2}E(\lambda)\tau_o(\lambda)\tau_a(\lambda)\rho(\lambda)\eta(\lambda)\lambda d\lambda \quad (6)$$

For the thermal infrared hyperspectral imager with spectral range between 3.0μm and 12.5μm, detection sensitivity can be represented by noise equivalent temperature difference NEΔT. Under laboratory conditions, system performance can be evaluated with black body. When ε=1, $\Delta\varepsilon$=0 and V_s=V_N, ΔT is equal to NEΔT. Considering the process factor of signal processing system, NEΔT can be formulated as (Xue, 1992):

$$\mathrm{NE}\Delta T=\frac{4\sqrt{A_D\Delta f}}{D_0^2\beta^2\delta_e\tau_o(\lambda)\tau_a(\lambda)D^*(\lambda)X_T(\lambda)} \quad (7)$$

where, $X_T(\lambda)$ represents differential radiant exitance, which is expressed as:

$$X_T(\lambda)=\int_{\lambda_1}^{\lambda_2}\frac{\partial L_T(\lambda)}{\partial T}d\lambda \quad (8)$$

2 NOISE MODEL OF HYPERSPECTRAL IMAGER

Overall noise of hyperspectral imager consists of noise in the time domain and noise in the spatial domain. Time-domain noise is related to each pixel of detector, which mainly includes inherent noise of detector, noise caused by signal electron fluctuations and the electronic noise. Spatial-domain noise is caused by the application of multi-element detector and focal plane detector and the occurrence of spectral dimension in hyperspectral imager and spatial factors like the non-uniformity and mutual superposition of different detector pixels and different wave bands can give rise to spatial-domain noise. In the analysis of traditional remote sense system, the analysis of time domain noise is clearer than that of spatial domain noise due to more extensive application of unit detectors. With extensive use of FPA in a new generation of hyperspectral imager, the influence of spatial domain noise on system performance becomes significant. Time domain noise and spatial domain noise are irrelevant, so total noise power of hyperspectral imager is equal to mean square root of time domain noise and spatial domain noise.

2.1 Time domain noise model

Time domain noise includes shot noise, readout noise, thermal noise, amplifier noise and so on. Essentially, this kind of noise is caused by random motion of micro particles, so it changes randomly with time. For hyperspectral imager with FPA, the system performance is mainly affected by the shot noise and the readout noise.

2.1.1 Shot noise

Photon fluctuation received by the photoelectric detector and the discontinuity and randomness of the photo-generated carriers' mobility will cause fluctuation of carriers and give rise to shot noise. Shot noise of hyperspectral imager mainly includes photon shot noise introduced by light-current I_S which is generated by the target radiation, photon noise of photocurrent I_P generated by other radiation (non-target radiation) and shot noise generated of FPA dark current I_{dark}. Spectral characteristics of these kinds of shot noise approximately approach to characteristics of the white noise, so in hyperspectral imager the total shot current noise can be expressed as:

$$i_N^2 = 2eI_d\Delta f = 2e[I_s + I_P + I_{dark}]\Delta f \quad (9)$$

where I_d is the sum of photocurrent generated by detector; e is the electronic charge and Δf is the system noise equivalent bandwidth. For FPA detetor with readout circuit, the Δf and the integration time of detector T_{int} have the following relation:

$$\Delta f = \frac{1}{2T_{int}} \quad (10)$$

According to Eq. (10) and Eq. (9), total number of electrons of shot noise is:

$$\begin{aligned} N_{shot} &= \frac{i_N \times T_{int}}{e} \\ &= \frac{1}{e} \times \sqrt{2eI_d\Delta f} \times T_{int} \\ &= \sqrt{N_s + N_P + N_{dark}} = \sqrt{N_d} \end{aligned} \quad (11)$$

Where N_d represents total number of signal electrons generated by the detector within the integration time T_{int}, which includes the number of photo-electrons N_S generated by target radiation, N_P generated by other radiation and N_{dark} generated by detector dark current. According to the current development level of hyperspectral imager, N_P generated by other radiation is affected by at least the following factors: the stray light of system, the background radiation of device, the response non-uniformity and the crosstalk of device, the superposition of spectral response functions in different wavebands and so on.

2.1.2 Readout noise

Readout noise N_{read} of FPA mostly arises from the inherent noise of device in readout circuit and additive noise introduced by the circuit structure or the operating mode. Readout noise mainly includes inherent noise and the switch noise of MOSFET and KTC noise. With the improvement of design and manufacturing process of FPA in recent years, the readout noise level has been greatly improved. In the visible and near-infrared waveband, readout noise of high-end CCD devices produced by some foreign manufacturers is as low as dozens of electrons. In the short-infrared waveband, the readout noise of HgCdTe FPA is also as low as several hundred electrons.

2.1.3 System signal-to-noise ratio

For hyperspectral imager with focal plane detector, the time-domain noise mainly includes two types of noises which are mentioned above. Because these two types of noises are irrelevant, total noise electrons of the system N_{total} can be expressed as:

$$N_{total} = \sqrt{{N_{shot}}^2 + {N_{read}}^2} \quad (12)$$

According to Eq. (4) and Eq. (11), after eliminating disable pixels of the detector, the calculating formula of system SNR based on quantum efficiency is:

$$SNR = \frac{N_s}{N_{total}} = \frac{N_s}{\sqrt{N_s + N_P + N_{dark} + {N_{read}}^2}} \quad (13)$$

According to the above formula, it can be seen that system SNR is limited by the number of readout noise electrons and the signal electrons generated by FPA. The signal electrons N_s are only a part of N_d, so:

$$SNR < \sqrt{N_s} \quad (14)$$

This formula shows that single pixel SNR of hyperspectral imager is limited by the square root of the total number of electrons collected by it. System SNR is not linear with the increase of signal, so the NE$\Delta\rho$ will change when the object has different reflectivity ρ. When ρ is relatively small, the sensitivity of system is relatively high. Fig.1 shows the relationship between single pixel output noise DN and the signal DN. It can be seen from this figure that when the signal is relatively small, system noise is mainly determined by the readout noise; when the signal increases gradually, system noise is predominated by shot noise and when signal is in saturated zone, the noise begins to fall again.

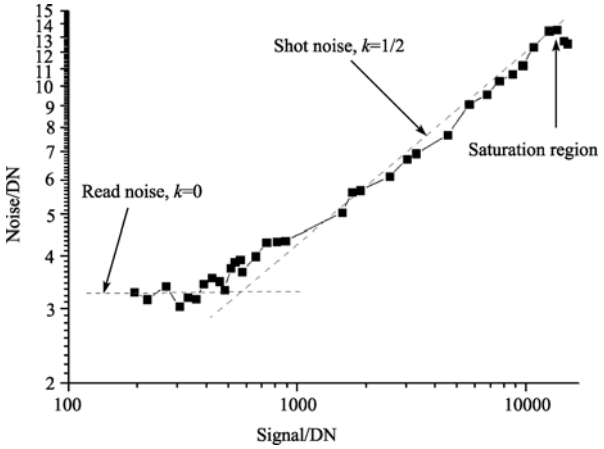

Fig. 1 Relationship between the noise DN and the signal DN of the SWIR FPA

2.2 Spatial-domain noise model

2.2.1 Non-uniformity noise of multi-unit detector

At present, most hyperspectral imagers use FPA detectors, so the impact of non-uniformity of the detector response on the system cannot be ignored. According to the National Standard of the People's Republic of China, the Technical Norms for Measurement and Test of Characteristic Parameters of Infrared Focal Plane Arrays (1998), the non-uniformity of IRFPA response U_R is defined as:

$$U_R = \frac{1}{\overline{R}} \sqrt{\frac{1}{M \times N - (d+h)} \sum_{i=1}^{M} \sum_{j=1}^{N} \left[R(i,j) - \overline{R} \right]^2} \quad (15)$$

where $R(i, j)$ is the responsivity of FPA pixel; M and N represent the number of rows and columns of FPA respectively; d and h are the number of non-responsive and excessively noisy pixels respectively. $\overline{R}$ is the average responsivity after eliminating the disabled pixels (including non-responsive and excessively noisy pixels). According to the current production level of FPA, response non-uniformity of CCD device is generally greater than 2%, while that of IRFPA is 5% or so. Because one

dimension of FPA of hyperspectral imager adopts spatial imaging and the other applies spectral imaging, non-uniformity in spatial image can be simplified to:

$$U_{\mathrm{R}}' = \frac{1}{\overline{R}}\sqrt{\frac{1}{N-p}\sum_{i=1}^{N-d}[R(i)-\overline{R}]^2} \tag{16}$$

where N is the number of pixels in spectral dimension; $\overline{R}$ is the average responsivity after eliminating the dead pixels in spectral dimension and p represents the number of dead pixels in spectral dimension. The non-uniformity of FPA can be improved through correction. Since there are a lot of methods for correcting non-uniformity, details of correction are not discussed here. In general, the non-uniformity of corrected hyperspectral images can be less than 1%. Fig.2 shows average DN value of each pixel before and after correction of non-uniformity of spectrogram in thermal infrared hyperspectral imager developed by SITP. This spectral channel's response non-uniformity is about 9.56% before correction, and it is reduced to about 0.24% after correction.

For single pixel, response non-uniformity of detector means different pixels have different responsivity, but for the whole remote sensing image, a kind of spatial domain noise is introduced. For hyperspectral imager, image noise in spatial domain introduced by response non-uniformity of detector is the product of non-uniformity and the average value of image. The electron number of spatial domain noise N_{R} introduced by response non-uniformity of the detector is formulated as:

$$N_{\mathrm{R}} = U_{\mathrm{R}}' \times N_{\mathrm{d}} \tag{17}$$

Spatial domain noise caused by detector response non-uniformity will change with changes of image signal, but for the linear response system the scale remains unchanged. Therefore, image non-uniformity constitutes the upper limit of image SNR. For instance, if the non-uniformity is 1%, the maximum image SNR cannot exceed 100. Therefore, reduction of system response non-uniformity plays a very important role in increasing radiant sensitivity of hyperspectral imager.

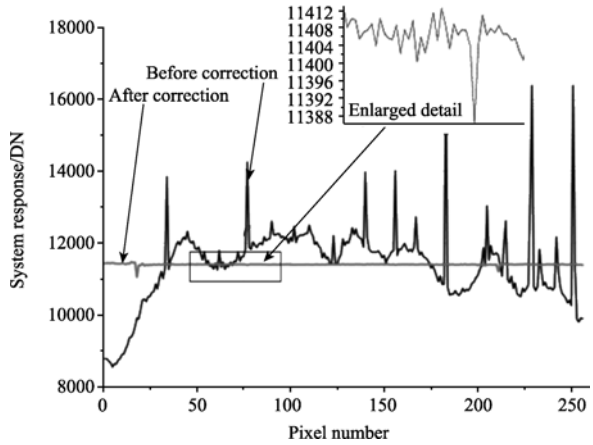

Fig. 2 Nonuniformity of a single channel before and after correction for a thermal infrared hyper-spectral imager

2.2.2 Spatial background radiation noise

Stray light of optical system and internal structure of hyperspectral imager and its own thermal radiation will also introduce noise and reduce radiation sensitivity of the system. In MWIR, LWIR and SWIR bands, hyperspectral imager that requires a long integration time is mainly influenced by the background infrared radiation. Especially for the thermal infrared hyperspectral imager, the signal generated by the system optical background radiation at room temperature greatly exceeds the radiation from the target itself. Background radiation becomes the main factor that restricts the improvement of system radiation sensitivity. Fig.3 shows the schematic diagram of infrared detector receiving background radiation.

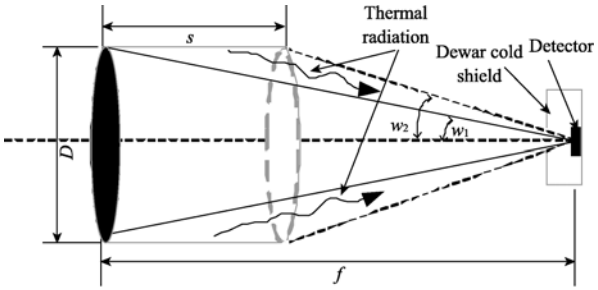

Fig. 3 Background thermal radiation model of the hyper-spectral imagery

In order to analyze the impact of background radiation of various components in the hyperspectral imager on system performance, the thermal radiation model shown in Fig.3 can be established. In the figure, ω_1 means the half field angle of detector dewar cold shield to the center of focal plane and ω_2 means the half field angle of the optical aperture to the center of the focal plane. The background thermal radiation can be divided into three parts, namely, dewar cavity thermal radiation, thermal radiation of the optical system and the structure background thermal radiation.

(1) Dewar cavity radiation

In order to reduce the influence of dewar cavity thermal radiation background of infrared detector, the cold shield is usually used to reduce thermal background. When aperture of cold shield coincides with the entrance pupil optical system (in Fig.3, $\omega_1=\omega_2$), that is, when f number of dewar cold shield exactly matches the optical system, the influence of thermal radiation on the system is the smallest and the thermal radiation of dewar cavity can be basically ignored. Sometimes, in order to simplify the system, cold shield is not designed for SWIR detector. Without cold shield, dewar cavity radiation will be directly received by the detector. The light current generated by SWIR thermal radiation of dewar cavity at room temperature is up to nearly pA level, which is equivalent to the detector dark current, so it can not be simply ignored here.

(2) Optical system thermal radiation

For influence of optical system radiation, besides target signal, the detector can also receive thermal background radiation generated

by optical lens or reflecting mirror. At room temperature, the background radiation from the optical system is much smaller than others in MWIR and SWIR, which can be ignored, while in the thermal infrared waveband, especially in the case that the detector's cold shield and the optical system matches perfectly, thermal background radiation of the optical system can not be ignored.

(3) Calculation of structure background thermal radiation

According to geometric relationship shown in Fig.3, when $\omega_1>\omega_2$, the background thermal radiation of the instrument cannot directly reach detector pixels, while its thermal radiation also will not reach pixels through other reflection paths. When $\omega_1<\omega_2$, thermal radiation of the instrument can be received directly by detector pixels, since inner wall of instrument is black treated, background thermal radiation must be taken into account seriously.

If P_b represents power of background thermal radiation received by detector pixel, similar to Eq.(5), the number of signal electrons N_{black} of light current generated by background thermal radiation can be expressed as:

$$N_{black} = N_{black}\eta = \frac{P_b T_{int}\lambda}{hc}\eta \tag{18}$$

As the background thermal radiation changes slowly with change of temperature of the instrument, such change can be removed through inter-calibration, but shot noise caused by background thermal radiation cannot be eliminated. Therefore, noises introduced by background thermal radiation and detector dark current are similar.

In addition to emissivity, radiation and temperature of object are closely related. Fig.4 shows the background radiation of the hyperspectral imager, which is designed by a project team in SITP, at different temperatures. In the process of system cooling down, the average irradiance of the detector photosensitive surface reduce from 7.24×10^{-4}W/cm^2 at 300K to 0.06×10^{-4}W/cm^2 at 150K, which is only 1/120 of the irradiance at 300K. Since the temperature plays an important role in the background radiation, cooling down the optical system is the most efficient method to reduce the background radiation.

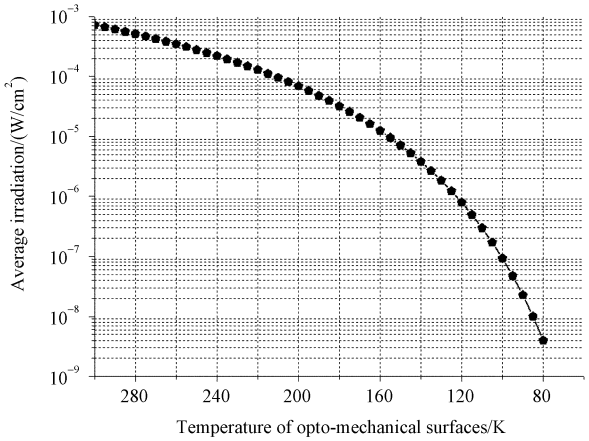

Fig. 4 Background radiation of the hyper-spectral imagery at different temperature

2.2.3 Stray light noise

For near-infrared or shortwave infrared band which mainly reflect sun signal, stray light is also an important factor for radiation sensitivity.

Though in the design system, non-target field signal will not be received by detector, the reflection rate of structure of the system to optical signal will not be absolute zero; thus signal outside the field will be in the images in form of stray light. Specially, when the light is strong, the impact of the stray light would be very serious. Since stray light changes with the targets and its surroundings, which is a random process can not be predicted, its direct performance in images is noise. Normally, stray light is associated with target surroundings, when the target background radiation is large, the effect of stray light will increase. For some particularly bright interfering signals (such as direct sunlight), special measures must be adopted for prevention.

2.2.4 Crosstalk of multi-unit detector

Pixel crosstalk of multi-unit detector may also affect the quality of hyperspectral images. For hyperspectral imaging system, pixel crosstalk in space-dimension of FPA will affect the image quality, mainly reflected by that the neighboring pixel signal is received by detector of the measured pixel. The influence of crosstalk is similar to the impact that optical system aberration decreases system spatial resolution, so the degradation of image quality caused by pixel crosstalk is more appropriate to be expressed with MTF of system. Pixel crosstalk in spectral dimension, which makes signals from different band superposing, then decreases spectral resolution. This problem will be discussed with the effects of spectrum aliasing on the radiation sensitivity. The problem that pixel crosstalk in spectral dimension makes signals from different band superpose and leads to decrease of spectral resolution and sensitivity of spectral superposing to system radiation will be discussed later together.

3 INFLUENCE OF SPECTRAL DIMENSION TO SYSTEM RADIATION SENSITIVITY

3.1 Influence of spectrum superposition

In hyperspectral imaging system, ideal waveband spectral response function $R(\lambda)$ should be a rectangular function (1992), whose center wavelength is λ_i and the bandwidth is $\Delta\lambda$. However, for an actual imaging system, the rectangular coefficient of the spectral response function will be worse due to the width of imaging slit, the optical system aberrations and the pixels crosstalk of multi-detector. The waveband spectral response function can be expressed with Gaussian function, thus spectral response function with the center wavelength of λ_i and the bandwidth of $\Delta\lambda$ can be expressed as (Wang & Xue, 1998):

$$R(\lambda) = \frac{1}{\sqrt{2\pi}\sigma} e^{-\frac{(\lambda-\lambda_i)^2}{2\sigma^2}} \tag{19}$$

Fig.5 shows that not only the target's signal in the spectral band is received by pixel, but also some signal whose wavelength is less than λ_i–1/2$\Delta\lambda$ or over λ_i+1/2$\Delta\lambda$ is received. These signals outside the band [λ_i–1/2$\Delta\lambda$, λ_i+1/2$\Delta\lambda$] lead to decrease of radiation sensitivity of spectral dimension.

Suppose the object's radiation power per wavelength is $P(\lambda)$, and the average radiation power in the band i [λ_i–1/2$\Delta\lambda$, λ_i+1/2$\Delta\lambda$] is $P\lambda_i$, according to Fig.5, the pixel response signal V_s in this band can be approximate expressed as :

$$\begin{aligned} V_S &= \int_0^{\infty} R(\lambda)P(\lambda)\mathrm{d}\lambda = \int_0^{\lambda i-\frac{1}{2}\Delta\lambda} R(\lambda)P(\lambda)\mathrm{d}\lambda + \\ &\int_{\lambda i+\frac{1}{2}\Delta\lambda}^{\infty} R(\lambda)P(\lambda)\mathrm{d}\lambda + P_{\lambda_i}\int_{\lambda i-\frac{1}{2}\Delta\lambda}^{\lambda i+\frac{1}{2}\Delta\lambda} R(\lambda)\mathrm{d}\lambda \\ &= \int_0^{\lambda i-\frac{1}{2}\Delta\lambda} R(\lambda)(P(\lambda)-P_{\lambda_i})\mathrm{d}\lambda + \\ &\int_{\lambda i+\frac{1}{2}\Delta\lambda}^{\infty} R(\lambda)(P(\lambda)-P_{\lambda_i})\mathrm{d}\lambda + \\ &P_{\lambda_i}\int_0^{\infty} R(\lambda)\mathrm{d}\lambda \end{aligned} \tag{20}$$

For different objects, $(P(\lambda)-P_{\lambda i})$ in Eq.(20) is a random number, the item 1 and 2 in Eq.(20) are the response outside the band i [λ_i–1/2$\Delta\lambda$, λ_i+1/2$\Delta\lambda$], which are equivalent to the noise, while the item 3 is the signal part proportional to $P_{\lambda i}$.

For the Gaussian function, the superposition of signals is mainly from near back and forth wave. If the reflectivity difference of the adjacent object band is less than 5%, and then the noise introduced by the superposition is about 1.2% of the signals through calculation. The above analysis is based on that the superposition of adjacent band's spectral response function is at the ideal 50% place, if the overlapped place become larger due to the optical aberration or others reasons, then the superposition noise introduced will be greater. This spectral superposition noise is a kind of spatial-domain noise caused by the system features, the mechanism of which and the test method are more complicated compared to other spatial noises like detector non-uniformity or noise generated by the background radiation.

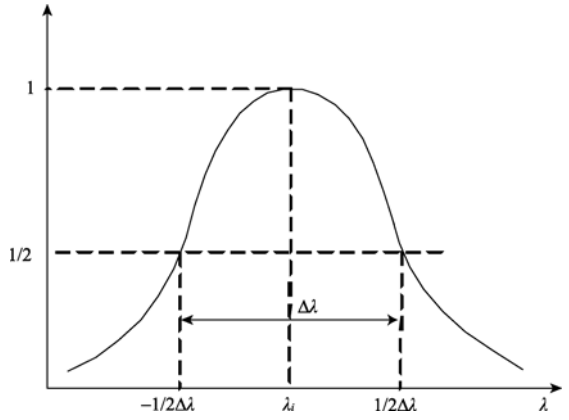

Fig. 5 Spectrum response function of the hyperspectral imagery simulated with Gaussian Function

3.2 Influence of consistency of radiation sensitivity in different waveband

The most prominent feature of hyperspectral imaging system is obtaining spatial and spectral information simultaneously. However, considering the non-uniformity of the solar radiation or target spectral radiation, spectral transmittance of optical system, detector spectral response and other factors. Especially different spectroscopic methods make the bandwidth of different wavebands different, many systems normally need to limit aperture and integral time to ensure fidelity of original data, which makes part of spectral waveband be weak and signal-noise ratio be low.

Ultimately each wave band's SNR of hyperspectral imaging are very different. The difference will affect the application effect directly if the dynamic scope of the system is limited, which makes a lot of wave bands not able to meet the application requirement. It is also the great concerning issue for the remote sensing consumers.

Consistency of radiation sensitivity in different wave bands is also an important factor needs to be very concerned (Bin, 1998). Generally, consistency of radiation sensitivity in different wave bands can be realized by choosing uniform dispersive component, applying different spectral resolution at different wave band.

Fig.6 illustrates the SNR curve of one SWIR hyperspectral imaging system based on the prismatic light splitting method, which is developed by SITP. Due to the refraction characteristics of the quartz dispersive prism, the bandwidth in the spectral range of 1.0—2.0μm is very wide, which is about 25—30nm; while in the spectral range of 2.0—2.5μm is narrow, which is about 16—25nm. However, solar radiation in the spectral range of 2.0—2.5μm is much weaker than that of range of 1.0—2.0μm, and therefore, SNR in the two spectral range are much different. The designer has solved this problem, namely, how to ensure the consistency of radiation sensitivity in different wave bands by the on-chip programming technology.

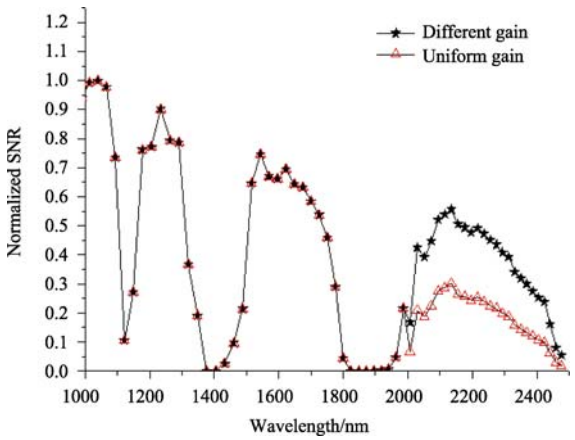

Fig. 6 Contribution of gain design of detector to improvement of SNR

By the on-chip programming, the corresponding detector gain for 2.0—2.5μm spectral range can be set as 4 times of 1.0—2.0μm spectral range, which will reduce the readout noise of detector in these wavebands and double the SNR, and then keep the consistency of sensitivity in different bands.

4 CONCLUSION

Radiation sensitivity is one of the most important parameters for hyperspectral imaging system. The paper analyzes the noise sources and characteristics of hyperspectral imaging system according to radiation characteristics and sensitivity calculation formula of objects, establishes noise models such as time-domain noise, spatial-domain noise, spatial interference and spectrum superposition, analyzes the influence of various noise to the sensitivity of hyperspectral imaging system and concludes that:

(1) Traditional analyzing method for SNR of hyperspectral imaging system holds that the system noise is mostly time-domain noise; however, with the development of hyperspectral imager and widely application of FPA detectors, the exist of spatial-domain noise gradually becomes the main limits of the system SNR, while it is more suitable to apply equivalent electron to calculate SNR now.

(2) The system sensitivity does not increase linearly with the object's reflectivity. When the target's reflectivity is low, $NE\Delta\rho$ is comparatively small, but the sensitivity is comparatively high, limit of the system's SNR is the square root of signal electron number.

(3) The analysis and calculation to noise introduced by the spatial-domain noise and spectral superposition show that the influence of noise to sensitivity can not be ignored, even it has been bottleneck restricting radiation sensitivity of hyperspectral imaging system.

REFERENCES

Shanghai Institute of Technical Physics. 1998. The Technical Norms for Measurement and Test of Characteristic Parameters of Infrared Focal Plane Arrays. GB/T17444-1998. Shanghai

Tong Q X, Zhang B and Zheng L F. 2006. Hyperspectral Remote Sensing: Principle, Technology and Application, Beijing: Higher Education Press

Wang J Y and Xue Y Q. 1992. 64-band airborne imaging spectrometer. *Journal of Infrared and Millimeter Waves*, **11**(3): 181—188

Xue Y Q. 1992. The technical development of airborne scan imaging systems. *Journal of Infrared and Millimeter Waves*, **11**(3): 169—180

Xiang L B, Zhao B C and Xue M Q. 1998, Spatially modulated imaging interferometry. *Acta Optica Sinica*, **18**(1): 18—22

Yu B X. 1995. Performance analysis of imaging spectrographs. *Optics Intelligence*, (Supplement), 1—19

高光谱成像系统的噪声模型和对辐射灵敏度的影响

王建宇[1], 王跃明[2], 李春来[2]

1.中国科学院 上海分院 上海 200083;
2.中国科学院 上海技术物理研究所 上海 200083;

摘 要: 高光谱成像系统的应用效果非常依赖仪器获取图像的信噪比。根据高光谱成像系统的设计特点和各种噪声的来源, 建立了时域噪声、空域噪声、空间干扰和光谱混叠等各种噪声模型, 在此基础上详细分析了各种噪声对高光谱成像系统的影响和制约, 结论对提升中国高光谱成像系统的实用性具有重要意义。

关键词: 高光谱, 辐射灵敏度, 噪声模型

中图分类号: TP702 文献标识码: A

引用格式: 王建宇, 王跃明, 李春来. 2010. 高光谱成像系统的噪声模型和对辐射灵敏度的影响. 遥感学报, **14**(4): 607—620
Wang J Y, Wang Y M and Li C L. 2010. Noise model of hyperspectral imaging system and influence on radiation sensitivity. *Journal of Remote Sensing*. **14**(4): 607—620

1 高光谱成像系统的辐射灵敏度计算的理论模型

评价高光谱成像系统的主要技术指标包括光谱分辨率和光谱覆盖范围、空间分辨率和空间覆盖范围以及系统辐射灵敏度等参数, 各个指标之间是相互制约的(童庆禧等, 2006)。成像系统在满足光谱分辨覆盖和空间分辨覆盖的指标要求之后, 能够达到的辐射灵敏度就是决定系统设计成败的关键。

本文通过对地物目标的辐射特征和系统辐射灵敏度方程的分析, 详细论述了各种噪声对系统辐射灵敏度的影响和制约, 特别是对空域噪声、光谱维的信号混叠以及波段间的不一致性对系统灵敏度的影响作了深入的研究。

1.1 地物目标的辐射特征

地物目标的辐射能量由对太阳光的反射和目标自身的热辐射两部分组成。光谱范围在 0.4—2.5μm 的可见光到短波红外波段, 地物目标辐射的主要能量是对太阳辐射的反射, 本身的热辐射相对较小, 计算时可以忽略; 在 3.0—5.0μm 和 8.0—12.5μm 之间的中、长波热红外波段, 地物目标对太阳辐射的反射能量相对较小, 此时地物目标辐射的主要能量以自身的热辐射为主。

对于具有朗伯反射体特性、反射率为 $\rho(\lambda)$的地物目标, 在可见光波段和短波红外波段进入高光谱成像系统探测器的单位波长光辐射功率 $P(\lambda)$可以表示为(禹秉熙, 1995):

$$P(\lambda)=\frac{\pi D_0^2}{4}\times\beta^2\times\tau_{\mathrm{o}}(\lambda)\times\left(\frac{1}{\pi}E(\lambda)\sin\theta\rho(\lambda)\tau_{\mathrm{a}}(\lambda)+L_{\mathrm{a}}(\lambda)\right) \tag{1}$$

式中, $E(\lambda)$表示太阳辐射在地面的光谱辐射照度, $\tau_{\mathrm{a}}(\lambda)$为大气光谱透过率, $\tau_{\mathrm{o}}(\lambda)$为仪器光学系统的总透过率, θ 表示太阳高度角, $L_{\mathrm{a}}(\lambda)$为由大气散射引起的程辐射度, D_0 为光谱仪的光学有效口径, β 为仪器的瞬时视场。为简单起见, 以下讨论中不考虑由大气散射引起的程辐射度 $L_{\mathrm{a}}(\lambda)$的影响。

对于地物目标的热辐射, 成像系统的目标和背景往往是相互的, 对辐射图像起作用的是景物像元的温度为 T, 比辐射率为 ε, 反射率为 ρ 与相邻像元的温度差 ΔT, 比辐射率差 $\Delta\varepsilon$ 和反射率差 $\Delta\rho$, 此时相邻像元的分谱辐射功率差$\Delta P(\lambda)$可以表示成(薛永祺, 1992):

收稿日期: 2010-02-05; 修订日期: 2010-05-01
基金项目: 中国科学院知识创新工程。
第一作者简介: 王建宇(1959—), 男, 博士, 毕业于中国科学院上海技术物理研究所。目前主要从事高光谱成像系统和激光主动遥感方面的研究工作。E-mail: jywang@mail.sitp.ac.cn。

$$\Delta P(\lambda)=\frac{1}{4}D_0^2\beta^2\tau_{\mathrm{a}}(\lambda)\tau_{\mathrm{o}}(\lambda)\times\left(\varepsilon(\lambda)\frac{\partial L_T(\lambda)}{\partial T}\Delta T+L_{\mathrm{T}}(\lambda)\Delta\varepsilon(\lambda)\right) \tag{2}$$

式中, $L_{\mathrm{T}}(\lambda)$表示景物的谱辐射率。

1.2 高光谱成像系统辐射灵敏度计算方程

对于光谱范围在0.4—2.5μm的高光谱成像系统, 探测灵敏度可以用信噪比SNR或系统的噪声等效反射率差 NE$\Delta\rho$ 表示, NE$\Delta\rho$ 表示在系统信噪比为 1 的目标的反射率差。

1.2.1 基于 D^*的信噪比计算—比探测率法

基于 D^*的信噪比计算是通过探测器的比探测率来计算系统信噪比, 这种方法合适于传统的基于单元和多元光导型探测器的高光谱成像系统, 对于系统中心波长为 λ, 窄带光谱带宽为$\Delta\lambda$ 的波段, 信噪比 SNR 可以表示为(薛永祺, 1992):

$$\mathrm{SNR}(\lambda)=\frac{V_{\mathrm{S}}(\lambda)}{V_{\mathrm{N}}(\lambda)}=\frac{D_0^2\beta^2\delta_{\mathrm{e}}}{4\sqrt{A_{\mathrm{d}}\Delta f}}\times\tau_{\mathrm{a}}(\lambda)\tau_{\mathrm{o}}(\lambda)D^*(\lambda)E(\lambda)\sin\theta\rho(\lambda)\Delta\lambda \tag{3}$$

式中, $\tau_{\mathrm{o}}(\lambda)$, $\tau_{\mathrm{a}}(\lambda)$, $D^*(\lambda)$, $E(\lambda)$, $\rho(\lambda)$是取光谱带宽为 $\Delta\lambda$ 内的平均值, δ_{e} 表示信号过程因子, V_{N} 为探测器响应的噪声电压, $D^*(\lambda)$为探测器的归一化光谱探测率或比探测率, A_{d} 为探测器像元的面积, Δf 为探测器电子学噪声带宽。

1.2.2 基于量子效率的计算方法——等效电子法

等效电子法是通过计算探测器所产生的信号电子数和噪声电子数计算系统的信噪比, 这种方法比较适用于采用的 CCD 探测器或红外焦平面探测器的高光谱成像系统。这种方法将入射到探测器像元上的辐射功率 $P(\lambda)$转化成光子数 $N_{\mathrm{P}}(\lambda)$, 再由探测器的光谱量子效率 $\eta(\lambda)$得到探测器激发的信号电子数 $N_{\mathrm{S}}(\lambda)$, 系统信噪比为信号电子数和各种噪声电子数之和 $N_{\mathrm{total}}(\lambda)$的比值:

$$\mathrm{SNR}(\lambda)=\frac{N_{\mathrm{s}}(\lambda)}{N_{\mathrm{total}}(\lambda)} \tag{4}$$

其中信号电子数 $N_{\mathrm{S}}(\lambda)$又可以表示成:

$$N_{\mathrm{s}}(\lambda)=N_{\mathrm{P}}(\lambda)\eta(\lambda)=\frac{P(\lambda)T_{\mathrm{int}}\lambda}{hc}\eta(\lambda) \tag{5}$$

式中, h 为普朗克常数, c 为光速, T_{int} 表示探测器的积分时间, 将式(1)带入式(5)得到:

$$\mathrm{SNR}=\frac{N_{\mathrm{s}}(\lambda)}{N_{\mathrm{total}}(\lambda)}=\frac{D_0^2\beta^2\sin\theta T_{\mathrm{int}}}{N_{\mathrm{total}}\times 4hc}\times\int_{\lambda_1}^{\lambda_2}E(\lambda)\tau_{\mathrm{o}}(\lambda)\tau_{\mathrm{a}}(\lambda)\rho(\lambda)\eta(\lambda)\lambda\mathrm{d}\lambda \tag{6}$$

对于光谱范围在 3.0—12.5μm 的热红外高光谱成像系统, 探测灵敏度可以由系统的噪声等效温差 NEΔT 来表示, 在实验室条件下用黑体评价系统性能。当 ε=1, $\Delta\varepsilon$=0, V_{s}=V_{N} 时的 ΔT 就是 NEΔT, 考虑到信号处理系统中的过程因子, 可以得到 NEΔT 的公式(薛永祺, 1992):

$$\mathrm{NE}\Delta T=\frac{4\sqrt{A_{\mathrm{D}}\Delta f}}{D_0^2\beta^2\delta_{\mathrm{e}}\tau_{\mathrm{o}}(\lambda)\tau_{\mathrm{a}}(\lambda)D^*(\lambda)X_{\mathrm{T}}(\lambda)} \tag{7}$$

式中, $X_{\mathrm{T}}(\lambda)$ 表示目标的微分辐射出射度, 其表达式为:

$$X_{\mathrm{T}}(\lambda)=\int_{\lambda_1}^{\lambda_2}\frac{\partial L_{\mathrm{T}}(\lambda)}{\partial T}\mathrm{d}\lambda \tag{8}$$

2 高光谱成像系统的噪声模型

高光谱成像系统的总噪声由时域噪声和空域噪声两部分组成。时域噪声是和探测器每个像元相关的噪声, 主要包括探测器内部固有的噪声、信号电子涨落引起的噪声和电子噪声。空域噪声主要是由于高光谱成像系统中多元探测器和焦平面探测器的应用以及光谱维信息的出现引起, 不同探测器之间和不同波段之间的不均匀和相互的混叠等空间因素都会引入空域噪声。在传统遥感系统的分析中, 由于仪器大部分采用单元器件, 对时域噪声的分析比较清楚, 对空域噪声分析相对较少, 随着新一代高光谱成像系统中大量使用焦平面器件, 空域噪声对系统性能的影响变得显著起来。时域噪声和空域噪声是不相关的, 故高光谱成像系统的总噪声功率等于两类噪声的均方和。

2.1 时域噪声模型

时域噪声包括散粒噪声、读出噪声、热噪声和放大器噪声等。从本质上讲, 这类噪声都是由于微观粒子的无规则运动引起的, 随时间的变化是随机的。对于采用焦平面器件的高光谱成像系统, 影响系统性能的主要是散粒噪声和读出噪声。

2.1.1 散粒噪声

照射在光电探测器上的光子起伏及光生载流子流动的不连续性和随机性会形成载流子起伏变化, 引起散粒噪声。在高光谱成像系统中散粒噪声主要包括由入射的目标辐射产生的光电流 I_{S} 引起的光子散粒噪声、由系统接收到的其他辐射(非目标辐射)产生的光电流 I_{P} 引起的光子噪声和由焦平面器件暗电流 I_{dark} 引起的散粒噪声, 这几类散粒噪声的频谱特性近似符合白噪声特性, 在高光谱成像系统中总的散粒电流噪声可以表示如下:

$$i_N^2 = 2eI_d\Delta f = 2e[I_s + I_P + I_{dark}]\Delta f \quad (9)$$

式中，I_d 为探测器产生的光电流总和，e 表示电子电荷点亮，Δf 表示系统的噪声等效带宽。对于带读出电路的焦平面探测器而言，其系统带宽 Δf 与探测器的积分时间 T_{int} 符合如下关系:

$$\Delta f = \frac{1}{2T_{int}} \quad (10)$$

将式(10)带入式(9)可以得到系统总的散粒噪声的电子数为:

$$N_{shot} = \frac{i_N \times T_{int}}{e} = \frac{1}{e} \times \sqrt{2eI_d\Delta f} \times T_{int} = \sqrt{N_s + N_P + N_{dark}} = \sqrt{N_d} \quad (11)$$

式中，N_d 表示探测器在积分时间 T_{int} 内产生的总信号电子数，它包括由入射目标辐射产生的光电流引起的电子数 N_s、由其他辐射产生的光电流引起的电子数 N_P 和由探测器暗电流产生的电子数 N_{dark}。根据目前高光谱成像系统的研制水平，这里的由其他辐射产生的电子数 N_P 至少与系统的杂散光、仪器的背景辐射、器件的响应非均匀性和串音以及各波段光谱响应函数的混叠等因素的影响。

2.1.2 读出噪声

焦平面器件的读出噪声 N_{read} 的主要来源于读出电路中所用器件的固有噪声和由电路结构和工作方式引入的附加噪声。读出噪声主要包含 MOS 管的固有噪声、MOS 管的开关噪声和 KTC 噪声，近年来随着焦平面探测器设计水平和制造工艺的提高，读出噪声水平得到了很大程度的改善。在可见近红外波段，国外部分厂家的高端 CCD 器件的读出噪声低至几十个电子，在短波红外波段，HgCdTe 焦平面器件的读出噪声也低至数几百个电子。

2.1.3 系统信噪比

对于采用焦平面探测器的高光谱成像系统，时域噪声主要是上述两部分噪声的总和，由于这两类噪声是不相关的，系统总的噪声电子数 N_{total} 可以表示为:

$$N_{total} = \sqrt{{N_{shot}}^2 + {N_{read}}^2} \quad (12)$$

将上式带入式(4)并结合式(11)，在剔除器件的坏点后，可以得到基于量子效率的系统信噪比计算公式为:

$$SNR = \frac{N_s}{N_{total}} = \frac{N_s}{\sqrt{N_s + N_P + N_{dark} + {N_{read}}^2}} \quad (13)$$

从上式可以看出系统的信噪比受限于读出噪声电子数的大小和焦平面激发的电子数大小，由于信号电子数 N_s 只是 N_d 的一部分，所以有:

$$SNR < \sqrt{N_s} \quad (14)$$

上式表明高光谱成像系统单个像元的信噪比受限于它所收集到的总电子数的开方，由于系统的信噪比并不随着信号的增加成线性关系，所以在不同的反射率 ρ 下 NE$\Delta\rho$ 也会随之变化，当 ρ 比较小的时候，相对灵敏度较高。图 1 给出了实际测量得到的某短波红外焦平面器件中单个像元在不同的信号的 DN 值时输出和噪声 DN 值。从图中可以看出在信号较小时，系统噪声主要由读出噪声决定，当信号逐渐增加，系统噪声中散粒噪声占主要成分，当信号处于饱和区时，噪声又开始下降。

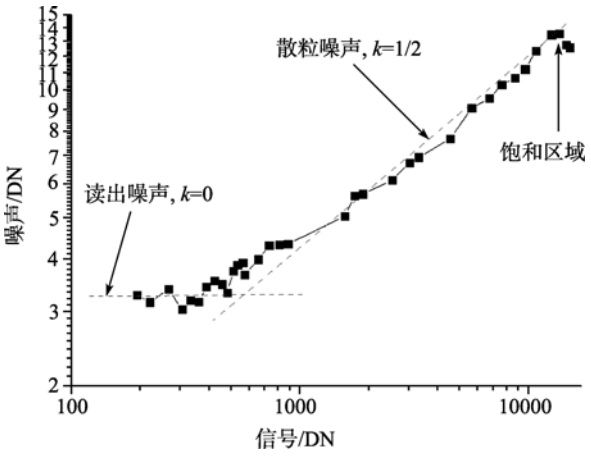

图 1 短波红外焦平面器件噪声 DN 值与信号 DN 值的关系

2.2 空域噪声模型

2.2.1 多元器件非均匀性噪声

目前主流的高光谱成像系统多采用焦平面阵列探测器，此时器件的响应非均匀性对系统的影响就变得不可忽视，根据中华人民共和国国家标准《红外焦平面阵列特性参数测试技术规范》(1998)，红外焦平面器件响应的不均匀性 U_R 的定义如下:

$$U_R = \frac{1}{\overline{R}}\sqrt{\frac{1}{M \times N - (d+h)}\sum_{i=1}^{M}\sum_{j=1}^{N}\left[R(i,j) - \overline{R}\right]^2} \quad (15)$$

式中，$R(i,j)$表示焦平面像元的响应率，M 和 N 表示焦平面器件的行数和列数，d 和 h 分别为死像元数和过热像元数。$\overline{R}$ 表示器件剔除坏点(包括死像元与过热像元)后的平均响应率。根据目前焦平面器件制造水平，CCD 器件的响应非均匀性一般优于 2%，红外焦

平面器件的响应非均匀性在 5%左右。由于高光谱系统的焦平面器件的一维是空间成像，另一维是光谱成像，所以在空间图像上的非均匀性可简化为：

$$U_R' = \frac{1}{\overline{R}}\sqrt{\frac{1}{N-p}\sum_{i=1}^{N-d}[R(i)-\overline{R}]^2} \tag{16}$$

式中，N 表示焦平面在光谱维上的像元数，$\overline{R}$ 表示器件光谱维剔除坏点后的平均响应率，p 表示光谱维上的坏点个数。焦平面器件的非均匀性可以通过校正得到改善，非均匀性校正的方法很多，这里不作介绍。一般来说，校正后的高光谱图像的非均匀性可小于 1%。图 2 是中国科学院上海技术物理研究所研制的一套热红外高光谱成像系统中某一波段光谱图像非均匀性校正前后的每个像元 DN 平均值分布。该光谱通道校正前响应的非均匀性约为 9.56%，校正后响应的非均匀性降低到约 0.24%。

器件的响应非均匀性对单个像元，只不过是不同像元的响应率有所不同而已，但对整个遥感图像，就是引入了一份噪声，只不过该噪声是以空域的形式存在。对于高光谱成像系统，器件的响应非均匀性引入的空间图像噪声为非均匀性和图像平均值的乘积，如果用噪声电子数 N_{R} 来表示，就是由器件的响应非均匀性引入的空间噪声电子 N_{R} 可以表示成：

$$N_{\mathrm{R}} = U_{\mathrm{R}}' \times N_{\mathrm{d}} \tag{17}$$

由器件响应非均匀性引起的空间噪声将随着图像信号的变化而变化，但对于线性响应系统其比例保持不变，因此图像非均匀性构成了图像信噪比的上限。例如，如果非均匀性为 1%时，图像的信噪比最大不可能超过 100。降低系统的响应非均匀性，对提高高光谱成像系统的辐射灵敏度十分重要。

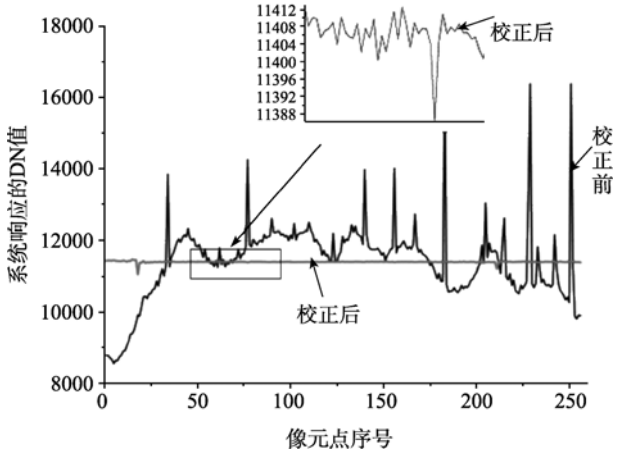

图 2　某热红外高光谱成像系统单通道校正前后的非均匀性对比

2.2.2　空间背景辐射噪声

高光谱成像系统的光学系统和内部结构的杂散光以及自身的热辐射也会给系统引入噪声，降低系统的辐射灵敏度。对于中、长波红外波段和短波红外波段需要较长积分时间的高光谱成像系统，主要受到背景红外辐射的影响。特别是对于热红外的高光谱成像系统，探测器对室温下仪器光机系统背景辐射产生的信号将大大超过地物目标产生的信号，成为限制系统辐射灵敏度提高的主要因素。

为了分析高光谱成像系统各部件的背景辐射对系统的性能影响，可以建立如图 3 的镜筒热辐射模型，图 3 中 ω_1 表示探测器杜瓦冷屏对焦面中心的半张角，ω_2 表示光学口径对焦面中心的半张角。背景热辐射主要可分为杜瓦腔体热辐射、光学系统热辐射和结构背景热辐射 3 个部分。

(1)　杜瓦腔体辐射

为了减少红外探测器杜瓦腔体热辐射背景的影响，一般通过设置冷屏来减少热背景。当冷屏的窗口和光学系统的入瞳完全重合(图 3 中 $\omega_1=\omega_2$)，即杜瓦冷屏 f 数与光学系统完全匹配时热辐射对系统的影响最小，使得杜瓦腔体的热辐射可以忽略。有时为了简化系统，对短波红外系统探测器并不设计冷屏。由于没有冷屏设计，杜瓦腔体的辐射将直接被探测器所接收，常温下，短波红外波段杜瓦腔体热辐射所产生的光电流也达接近皮安培量级，与探测器暗电流相当，此时就不能简单忽略了。

(2) 光学系统热辐射

探测器所接收到的除目标信号外，还有光学透镜或反射镜本身产生的热背景辐射。在常温下，光学系统在中、短波红外波段所产生的背景辐射相比于其他背景可以忽略，但到热红外波段，特别是在探测器的冷光栏和光学系统不能很好匹配的时候，光学系统本身的热背景就不能再忽略了。

(3)　结构背景热辐射计算

从图 3 的几何关系可以看出当 $\omega_1>\omega_2$ 时，仪器结构镜筒的背景热辐射是不可能直接达到探测器像元的，则此时它的热辐射不会通过其他反射路径到达探测元。当 $\omega_1<\omega_2$ 仪器镜筒热辐射就能到达探测像元，由于仪器镜筒内壁一般经过发黑处理，这时仪器镜筒产生的背景热辐射就必须考虑了。

如果用 P_{b} 表示背景热辐射到达探测元的功率，那么类似式(5)可以得到由背景热辐射产生的光电流引起的信号电子数 N_{black} 为：

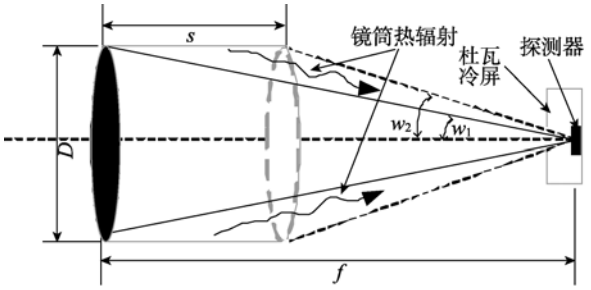

图 3 高光谱成像仪镜筒背景热辐射模型图

$$N_{\text{black}} = N_{\text{black}}\eta = \frac{P_{\text{b}}T_{\text{int}}\lambda}{hc}\eta \tag{18}$$

由于背景热辐射是随仪器的温度变化而变化的缓变过程，这类变化可以通过定标加以去除，但背景热辐射产生的电子数引入散粒噪声并无法消除，所以对于背景热辐射产生的噪声和探测器的暗电流引入的噪声类似。

除发射率以外，物体的辐射与温度也密切相关。图 4 给出了中国科学院上海技术物理研究所为某项目研制的一套热红外高光谱成像系统在不同环境温度下探测器接收的背景辐射曲线。在仪器光机系统降温的过程中，探测器光敏面上的平均辐照度由 300K 时的 7.24×10^{-4}W/cm^2 降低到 150K 时的 0.06×10^{-4}W/cm^2，约降低至 300K 时的 1/120。温度对背景辐射的影响很大，所以对光机系统进行制冷是抑制系统背景辐射的最有效方法。

2.2.3 杂散光噪声

对于可见近红外和短波红外这种以反射太阳信号为主的波段，杂散光也是影响高光谱成像系统辐射灵敏度的一个重要因素。尽管在系统设计中，非目标视场的信号不会进入对应的探测器，但由于系统的结构对光学信号的反射率不可能绝对为零，这样对于视场以外的信号就会以杂散光的形式出现的图像中，特别当出现强光时，杂散光的影响会变得相当严重。由于杂散光的产生随目标和目标周边的情况而变化，是一个无法预测的随机过程，因此在图像中的直接表现就是噪声。一般情况下，杂散光和目标环境相关，当目标背景辐射亮度大的时候，杂散光的影响也会增加，对于一些特别亮的干扰信号(如太阳光的直射)，则系统必须采用专门的措施来防护。

2.2.4 多元器件的串音噪声

多元探测器像元之间的串音也会影响高光谱图像的质量。对高光谱成像系统来说，焦平面器件空间

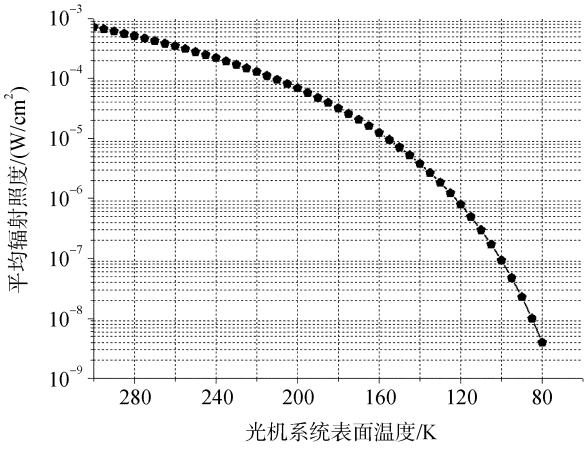

图 4 不同光机系统表面温度对应的仪器背景辐射

维像元之间的串音会影响空间图像的质量，主要表现为邻近像元的信号进入了被测像元的探测器中。串音对系统的影响效果与光学系统像差使系统空间分辨率下降的效果类似，所以像元之间串音引起的图像质量退化，用系统的 MTF 特征来描述更为合适。对于光谱维像元之间的串音，会让不同波段的信号混叠，使得波段的光谱分辨率下降，该问题将和下面的光谱混叠对系统辐射灵敏度的影响一并讨论。

3 光谱维对系统辐射灵敏度的影响

3.1 光谱混叠的影响

在高光谱成像系统中，理想的波段光谱响应函数 $R(\lambda)$应该是一个中心波长为 λ_i，波长带宽为 $\Delta\lambda$ 的矩形函数。但实际的系统由于成像狭缝的宽度、光学系统的像差以及多元探测器像元之间的串音会使得仪器光谱响应函数的矩形系数变差。在实际应用中波段的光谱响应函数可以用高斯函数来表示，对于中心波长为 λ_i，波长带宽为 $\Delta\lambda$ 的光谱响应函数可用高斯函数表示为(王建宇 & 薛永祺, 1992) :

$$R(\lambda) = \frac{1}{\sqrt{2\pi}\sigma}\mathrm{e}^{-\frac{(\lambda-\lambda_i)^2}{2\sigma^2}} \tag{19}$$

从图 5 的光谱响应函数曲线看到，不但光谱波段 $\Delta\lambda$ 内的目标信号被对应该波段的探测元接收，对于波长小于 λ_i–1/2$\Delta\lambda$ 和波长大于 λ_i+1/2$\Delta\lambda$ 部分信号同样会进入该波段的探测元，这些波段外的信号使得系统对光谱维探测的辐射灵敏度下降。

设地物的波长光辐射功率为 $P(\lambda)$，用 $P_{\lambda i}$ 表示地物在系统探测第 i 波段[λ_i–1/2$\Delta\lambda$, λ_i+1/2$\Delta\lambda$]内波长光辐射功率的平均值，结合图 5 得到该波段的探测元

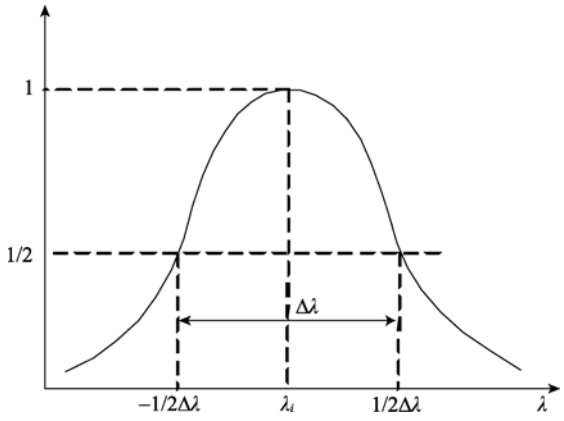

图 5　高斯函数模拟的光谱响应函数

的响应信号 V_s 可近似表示为:

$$V_s=\int_0^{\infty}R(\lambda)P(\lambda)\mathrm{d}\lambda=\int_0^{\lambda i-\frac{1}{2}\Delta\lambda}R(\lambda)P(\lambda)\mathrm{d}\lambda+\int_{\lambda i+\frac{1}{2}\Delta\lambda}^{\infty}R(\lambda)P(\lambda)\mathrm{d}\lambda+P_{\lambda_i}\int_{\lambda i-\frac{1}{2}\Delta\lambda}^{\lambda i+\frac{1}{2}\Delta\lambda}R(\lambda)\mathrm{d}\lambda$$
$$=\int_0^{\lambda i-\frac{1}{2}\Delta\lambda}R(\lambda)(P(\lambda)-P_{\lambda_i})\mathrm{d}\lambda+\int_{\lambda i+\frac{1}{2}\Delta\lambda}^{\infty}R(\lambda)(P(\lambda)-P_{\lambda_i})\mathrm{d}\lambda+P_{\lambda_i}\int_0^{\infty}R(\lambda)\mathrm{d}\lambda \tag{20}$$

对于不同的地物，上式中的$(P(\lambda)-P_{\lambda i})$是个随机数，式(20)中的第 1 项和第 2 项为波长带外的响应，相当于噪声，第 3 项是与 $P_{\lambda i}$ 成正比的信号部分。对于高斯函数，信号的混叠主要来源于相邻的前后波段，如果地物信号相邻波段之间的反射率差小于 5%，经计算由该混叠引入的噪声约为信号的 1.2%。以上分析的前提是相邻波段的光谱响应函数交叠在理想的 50%处，如因光学像差等原因引起交叠处变大，则引入的噪声会更大。这种光谱混叠引起的噪声是系统特性引入的一种空间噪声，相对于器件的非均匀性和系统的背景辐射等空间噪声，该噪声的机理和测试都更加复杂，但这也是高光谱成像系统所特有的，在将来的系统设计和研制中必须给予足够重视。

3.2　波段间辐射灵敏度一致性的影响

高光谱成像系统的最大特点是能够同时获取几何信息和光谱信息。但由于太阳辐射或目标光谱辐射亮度、光学系统光谱透过率、探测器光谱响应等参数的不均匀性影响，特别是不同的分光方法，使得不同波长的波段的带宽有很大的不同。很多系统为了确保原始数据不发生饱和失真，通常需要限制系统的孔径或积分时间，使得探测器接收的部分光谱波段信号很弱，信噪比较低，最终引起高光谱成像仪各波段图像数据的信噪比存在较大差别。这种差别在信息获取系统动态范围有限的条件下，直接影响系统的应用效果，使得很多波段不能够满足应用需求，这也是用户十分关心的问题。

波段间辐射灵敏度的一致性也是系统设计中需要十分关注的一个问题(相里斌等,1998)，一般可以通过选择均匀的色散元件、对不同波段选择不同的光谱分辨率、以及对不同的波段选用不同的增益来最终达到波段间辐射灵敏度的一致。

图 6 为中国科学院上海技术物理研究所研制的基于棱镜分光的短波红外高光谱成像系统波段信噪比曲线，由于受石英色散棱镜折射率特性决定，仪器在 1.0—2.0μm 光谱范围带宽较宽(约 25—30nm)，在 2.0—2.5μm 光谱范围带宽较窄(16—25nm)。太阳辐射在 2.0—2.5μm 光谱范围的辐射能量比在 1.0—2.0μm 光谱范围的辐射能量微弱得多，引起两个光谱段信噪比较大的差异。设计者通过红外焦平面片上编程技术解决了如何确保系统的波段灵敏度一致性这一难题。通过片上编程技术，将 2.0—2.5μm 光谱范围对应的探测器增益设置为 1.0—2.0μm 光谱范围的 4 倍，减小了这些波段的探测器读出噪声，将信噪比提高了约 1 倍，使各波段获得了很好的灵敏度一致性。

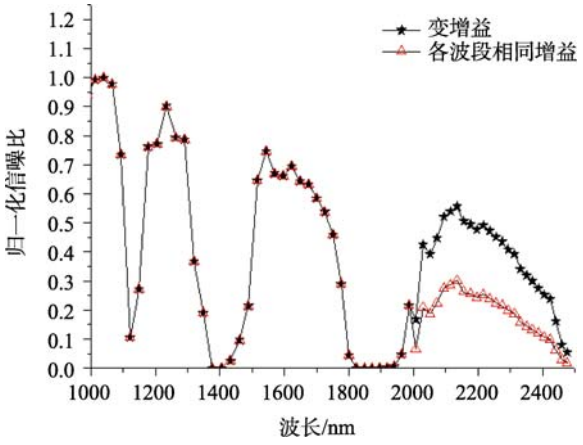

图 6　探测器变增益设计对改善波段信噪比一致性的贡献

4　结　论

辐射灵敏度是高光谱成像系统最重要的技术指标之一，本文根据地物目标的辐射特性和灵敏度计

算方程，分析了高光谱成像系统中的各种噪声来源和特点，建立了时域噪声、空域噪声、空间干扰和光谱混叠等各种噪声模型，并详细分析了各种噪声对高光谱成像系统灵敏度的影响，得到以下结论:

(1) 传统方法分析高光谱成像系统的信噪比认为系统的主要噪声是时域噪声，随着高光谱成像系统的发展和面阵焦平面器件的广泛应用，空域噪声的存在成了限制系统信噪比的主要因素，此时的系统信噪比计算方法以等效电子法计算更加合适。

(2) 系统的灵敏度不随地物反射率的增加而线性增加。当目标反射率低的时候，NE$\Delta\rho$ 也较小，但相对灵敏度较高，系统信噪比的极限是信号电子数的 1/2 次方。

(3) 通过对空域噪声和光谱混叠引入的噪声的分析和计算表明，这些噪声对系统的灵敏度的影响是不可忽视的，有时甚至可以成为制约高光谱成像系统辐射灵敏度的瓶颈。

REFERENCES

Shanghai Institute of Technical Physics. 1998. The Technical Norms for Measurement and Test of Characteristic Parameters of Infrared Focal Plane Arrays. GB/T17444-1998. Shanghai

Tong Q X, Zhang B and Zheng L F. 2006. Hyperspectral Remote Sensing: Principle, Technology and Application, Beijing: Higher Education Press

Wang J Y and Xue Y Q. 1992. 64-band airborne imaging spectrometer. *Journal of Infrared and Millimeter Waves*, **11**(3): 181—188

Xue Y Q. 1992. The technical development of airborne scan imaging systems. *Journal of Infrared and Millimeter Waves*, **11**(3): 169—180

Xiang L B, Zhao B C and Xue M Q. 1998, Spatially modulated imaging interferometry. *Acta Optica Sinica*, **18**(1): 18—22

Yu B X. 1995. Performance analysis of imaging spectrographs. *Optics Intelligence*, (Supplement), 1—19

附中文参考文献

红外焦平面阵列特性参数测试技术规范. 1998. 中华人民共和国国家标准. GB/T17444-1998. 上海

童庆禧，张兵，郑兰芬. 2006. 高光谱遥感:原理技术与应用. 北京: 高等教育出版社

王建宇，薛永祺. 1992. 64 波段机载光谱成像仪. 红外与毫米学报, **11**(3): 181—188

薛永祺. 1992. 机载扫描成像系统的技术发展. 红外与毫米波学报, **11**(3): 169—180

相里斌，赵宝常，薛鸣球. 1998, 空间调制干涉成像光谱技术. 光学学报, **18**(1): 18—22

禹秉熙. 1995. 成像光谱仪的性能分析. 光机情报, (增刊): 1—19